01 Jun 1993 - 06 Jun 1993

Practical Studies of the Seismic Response of a Rockfill Dam and a Tailings Impoundment

W. D. Liam Finn
University of British Columbia, Vancouver, British Columbia, Canada

Proceedings: Third International Conference on Case Histories in Geotechnical Engineering, St. Louis, Missouri, June 1-4, 1993, SOA 6

Practical Studies of the Seismic Response of a Rockfill Dam and a Tailings Impoundment

W. D. Liam Finn
Department of Civil Engineering, University of British Columbia, Vancouver,British Columbia, Canada

SYNOPSIS Two case studies from engineering practice are presented to demonstrate how useful a sophisticated finite element analysis can be in providing a comprehensive understanding of how dams behave during earthquakes. The first example involves determining, from the recorded performance of a rockfill dam, the volume change characteristics of the rockfill which cannot be measured directly. The second example covers the full range of current capability for analysis. It involves dynamic effective stress analysis of a tailings dam to check the triggering of liquefaction and the analysis of post-liquefaction flow deformations.

INTRODUCTION

The purpose of this paper is to demonstrate the important wide-ranging contributions that a comprehensive dynamic finite element analysis can make to understanding the performance of earth structures under earthquake loading. A comprehensive method of analysis is one that has the capability to model the important phenomenological aspects of response. These aspects are nonlinear hysterestic stress-strain behaviour, volumetric compaction or dilation, the development of seismic porewater pressures and the adaptation of response to the changing effective stress environment. The utility of a comprehensive method will be demonstrated by two examples from engineering practice.

The first example relates to the performance of the Matahina Dam in New Zealand during the 1987 Edgecumbe earthquake. This rockfill dam was instrumented for the measurement of acceleration in a number of locations. Displacement monuments on the downstream slope were read shortly before and immediately after the earthquake and so provided a pattern of earthquake induced permanent displacements. The shaking from the Edgecumbe earthquake was considerably less than that expected from the design earthquake. The owners were interested in estimating the performance under the design earthquake, using the measured response to the Edgecumbe earthquake as a check on the procedure for analysis. Useful estimates of the necessary material properties were available or could be measured in-situ with the exception of the volume change characteristics of the rockfill under dynamic straining. The challenge in this case was to solve the inverse problem; given the performance of the dam and all other necessary properties deduce the volume change characteristics of the rockfill. The only practical approach was the direct solution of the inverse problem.

The second example involves studies conducted as part of the seismic safety evaluation of the Original and Main tailings dams in the St. Joe State Park near Flat River, Missouri. The analysis focuses on the Original Dam and involves both dynamic effective stress analysis to investigate the triggering of liquefaction and analysis of the post-liquefaction flow deformations to assess the consequences of liquefaction. Therefore, this example involves the full range in present capability for the analysis of the earthquake behaviour of dams.

MATAHINA ROCKFILL DAM

The Matahina Dam (Fig. 1) was shaken strongly by the Edgecumbe earthquake of March 2, 1987 (Staff, NZ, DSIR, 1987). The earthquake had a local magnitude $M_L = 6.3$. The dam is located on the Rangatake River in the eastern Bay of Plenty Region of New Zealand about 23 km from the epicentre of the earthquake and about 11 km from the main surface rupture.

The dam is 86 m high with a crest length of 400 m. It has an upstream sloping core of weathered greywacke with a low plasticity gravelly clay grading. The dam shoulders are of hard ignimbrite rockfill compacted by heavy tractor track rolling. The transition zones between core and shoulders are comprised of the fines and soft

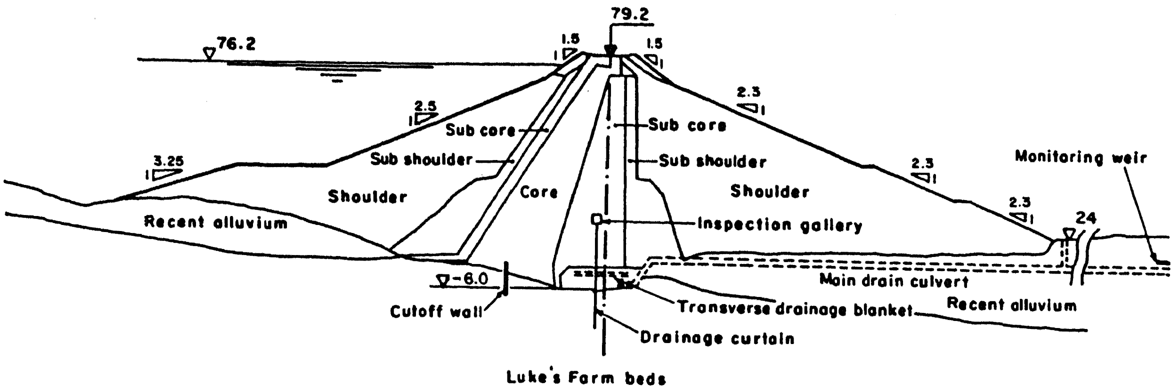

Fig. 1. Cross-Section of Matahina Dam.

ignimbrite stripping from the rockfill quarry and the excavations at the left abutment spur (Gillon and Newton, 1989).

The dam is well instrumented to record and observe the effects of earthquake loading. Accelerometers are located along the crest at the left and right abutments and at the centre. Along the centreline down the downstream shoulder, accelerometers are also located at approximately mid-height and in the foundation soils a few metres from the toe. Monuments are located along a number of lines on the downstream shoulder of the dam for the tracking of vertical and horizontal deformations. Measurements made on these monuments after the earthquake, yielded reliable estimates of permanent seismically induced deformations.

The Works & Development Services Corporation (NZ) Ltd. awarded a contract for an attempt at simulating the recorded response of Matahina Dam to the Edgecumbe earthquake using the nonlinear static and dynamic analysis program TARA-3 (Finn et al., 1986). If this response could be simulated satisfactorily, then consideration would be given to analyzing the response of the dam to an earthquake with a magnitude representative of a suitable design earthquake of greater magnitude than the Edgecumbe earthquake.

Major positive factors for the study were the high quality and detailed nature of the post-earthquake investigations. In particular the acceleration records (McVerry, 1987, 1989) and the displacement measurements (Gillon, 1988; Gillon and Newton, 1989) have been subjected to extensive critical evaluation. These evaluations have yielded reliable high quality data and the clear picture of events so essential to effective simulation.

On the negative side there was little information available on the dynamic properties of the core or of the static and dynamic properties of the rockfill. Shear wave velocity data in limited areas of the core and rockfill were obtained especially for this simulation study and were useful in estimating shear moduli (Sutherland and Logan, 1988). Volume changes in the rockfill contribute significantly to the seismic deformations of the dam but the parameters in the TARA-3 program controlling these cannot be measured directly because of the size of the rockfill. The parameters must be determined by the simulation process.

The following computational strategy was adopted for deriving the volume change characteristics of the rockfill from the field data. The strategy was based on the concept that the permanent seismic deformations of the dam were due to a combination of constant volume distortions and deformations due to volume change. The constant volume distortions result from the hysteretic nature of the response of soils and rockfill to seismic loading. The differences between the measured deformations of the dam and the constant volume deformations were attributed to volume changes in the rockfill. The distribution of volume changes necessary to match the measured deformations were calculated by solving the inverse problem of Matahina Dam. In a direct solution the volume change characteristics of the rockfill are known and the total deformations of the dam are computed. In the inverse problem, the deformations are known and the volume change characteristics of the rockfill are determined. This is possible at Matahina because of the rather complete specification of the deformations of the downstream shoulder. In summary, the measured displacement data of Matahina Dam are used to deduce the unknown volume change properties of the rockfill. These properties can then be used to compute the unknown displacements of Matahina Dam under excitation by an appropriate design earthquake. The response of this dam has been discussed previously by Finn et al. (1992).

SEISMICALLY INDUCED PERMANENT DEFORMATIONS

Measured vertical and horizontal components of seismically induced deformations along the centreline of the dam are shown in Fig. 2. These were measured on surface monuments on the downstream shoulder of the rockfill shell. A lower limit for the distortional deformations is obtained by a nonlinear dynamic analysis of the dam under conditions of zero volume change. The distortions are due to the residual deformations resulting from the hysteretic nonlinear response of the shoulders, sub-shoulders and the core. The differences between the measured displacements and the constant volume displacements at the monument locations are due to volume changes in the embankment materials and any purely surficial effects at the monument locations. The pattern of downstream shoulder deformations is in keeping with the location of the monuments and the geometry of the slope. Near the crest the slope is steeper, resulting in higher post-construction shear stresses and therefore lower tangent moduli. The accelerations are greatest in this location. The combination of low tangent moduli and high accelerations leads to substantially larger horizontal deformations.

TWO-DIMENSIONAL NONLINEAR ANALYSIS

The program TARA-3 developed by Finn et al. (1986) which was used to model the nonlinear response of Matahina Dam will be described briefly here.

Method of Analysis

An incremental approach has been adopted to model nonlinear behaviour using tangent shear and bulk moduli, G_t and B_t, respectively. The incremental dynamic equilibrium forces $\{\Delta P\}$ are given by

$$[M]\{\Delta\ddot{x}\} + [C]\{\Delta\dot{x}\} + [K]\{\Delta x\} = \{\Delta P\} \tag{1}$$

where [M], [C] and [K] are the mass, damping and stiffness matrices respectively, and $\{\Delta\ddot{x}\}, \{\Delta\dot{x}\}, \{\Delta x\}$ are the matrices of incremental relative accelerations, velocities and displacements. The viscous damping is of the Rayleigh type and its use is optional. Very small amounts of viscous damping are used, typically equivalent to less than 1% of critical damping in the dominant response mode. Its primary function is to control any high frequency oscillations that may arise from numerical integration. Damping is primarily hysteretic and is automatically included as the hysteretic stress-strain loops are executed during analysis.

The stiffness matrix is a function of the current tangent moduli during loading or unloading. The use of shear and bulk moduli allows the elasticity matrix $[\underline{D}]$ to be expressed as

$$[\underline{D}] = B_t[\underline{Q}_1] + G_t[\underline{Q}_2] \tag{2}$$

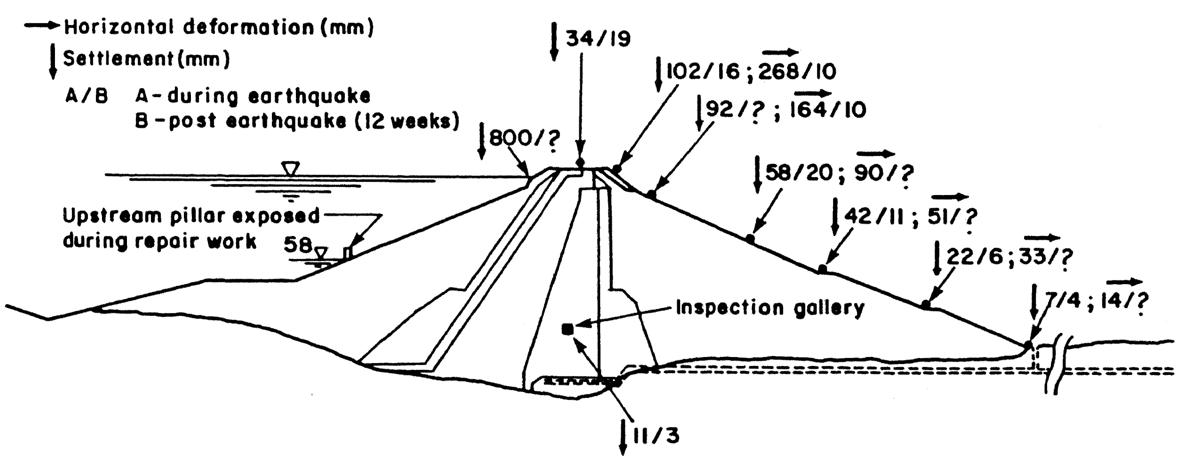

Fig. 2. Final Deformations at Centre of Matahina Dam.

where $[Q_1]$ and $[Q_2]$ are constant matrices for the plane strain conditions usually considered in analyses. This formulation reduces the computation time for updating $[\underline{D}]$ whenever G_t and B_t change in magnitude because of straining or porewater pressure changes.

Stress-Strain Behaviour in Shear

The behaviour of soil in shear is assumed to be nonlinear and hysteretic and exhibits Masing behaviour (1926) during unloading and reloading. Masing behaviour provides hysteretic damping.

The relationship between shear stress τ and shear strain γ for the initial loading phase under either drained or undrained loading conditions is assumed to be hyperbolic and given by

$$\tau = f(\gamma) = \frac{G_{max}\,\gamma}{(1 + (G_{max}/\tau_{max})|\gamma|)} \tag{3}$$

in which G_{max} is the maximum shear modulus and τ_{max} is the appropriate shear strength. This initial loading or skeleton curve is shown in Fig. 3(a). The unloading-reloading curves are modelled using the Masing criterion. This implies that the equation for the unloading curve from a point (γ_r, τ_r) at which the loading reverses direction, is given by

$$\frac{\tau - \tau_t}{2} = \frac{\dfrac{G_{max}(\gamma - \gamma_r)}{2}}{\left(1 + (\dfrac{G_{max}}{2\tau_{max}})\left|\gamma - \gamma_r\right|\right)} \tag{4}$$

or

$$\frac{\tau - \tau_r}{2} = f\left(\frac{\gamma - \gamma_r}{2}\right) \tag{5}$$

The shape of the unloading-reloading curve is shown in Fig. 3(b).

Finn et al. (1976) proposed rules for extending the Masing concept to irregular loading. They suggested that unloading and reloading curves follow the skeleton loading curve when the magnitude of the previous maximum shear strain is exceeded (Fig. 3c). When the current loading curve intersects the previous loading curve the stress-strain curve follows the previous loading curve (Fig. 3d).

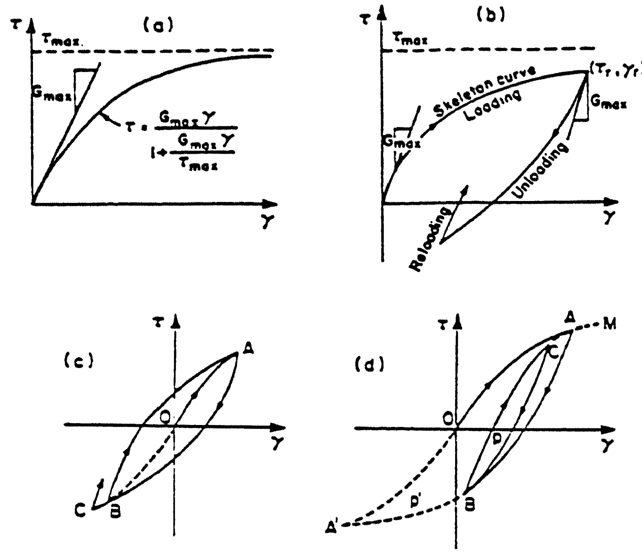

Fig. 3. Nonlinear Hysteretic Stress-Strain Paths.

The tangent shear modulus, G_t, for a point on the skeleton curve is given by

$$G_t = \frac{G_{max}}{\left(1 + \dfrac{G_{max}|\gamma|}{\tau_{max}}\right)^2} \tag{6}$$

At a stress point on an unloading or reloading curve G_t is given by

$$G_t = \frac{G_{max}}{\left(1 + \dfrac{G_{max}}{2\tau_{max}}\left|\gamma - \gamma_r\right|\right)^2} \tag{7}$$

Stress-Strain Behaviour in Hydrostatic Compression

The response of the soil to uniform all round pressure is assumed to be nonlinearly elastic and dependent on the mean normal stress. Hysteretic behaviour, if any, is neglected in this mode. The relationship between tangent bulk modulus, B_t, and mean normal effective stress, σ'_m, is assumed to be in the form

$$B_t = K_b P_a \left(\frac{\sigma'_m}{P_a} \right)^n \qquad (8)$$

in which K_b is the bulk modulus constant, P_a is the atmospheric pressure in units consistent with σ'_m, and n is the bulk modulus exponent.

Seismically induced porewater pressures are not included in the analysis of the response of Matahina Dam due to the Edgecumbe earthquake since no information is available on the pore pressure generation characteristics of the core material or on its liquefaction resistance. The response of the core will be analyzed in terms of total stresses. The displacements due to consolidation of the core are expected to be small during the time frame covered by the analysis.

VOLUME CHANGE CHARACTERISTICS

Under drained simple shear conditions, the volumetric strain increment $\Delta\varepsilon_{vd}$ is a function of the total accumulated volumetric strain ε_{vd} and the amplitude of the current shear strain γ (Martin, Finn and Seed, 1975). A convenient functional form proposed by Byrne (1991) is

$$\Delta\varepsilon_{vd} = \gamma C_1 \exp\left(-C_2 \frac{\varepsilon_v}{\gamma} \right) \qquad (9)$$

in which C_1 and C_2 are volume change constants that depend on the material type and relative density. For silts and sands, they may be determined directly by means of drained cyclic simple shear tests on dry or saturated samples (Martin, Finn and Seed, 1975) or inferred from field data on liquefaction resistance as described by Finn (1988). None of these options are available for rockfill.

Increments in porewater pressure, Δu, may be derived from the increments in volumetric strain using the equation

$$\Delta u = \overline{E}_r \Delta\varepsilon_{vd} \qquad (10)$$

where $\overline{E}_r$ is the effective stress dependent rebound modulus. Equation (10) is used in the second example to generate the time histories of porewater pressure.

In 2-D analysis in practice, the permanent volume changes due to shearing action are related to the cyclic shear stresses on horizontal planes because the seismic input motions are usually assumed to be shear waves propagating vertically. Therefore, in TARA-3, for computation of $\Delta\varepsilon_{vd}$ in equation (9), the shear strain on the horizontal plane, γ_{xy} is substituted in place of γ.

The distribution of volumetric strains in the finite elements representing the rockfill of Matahina Dam, calculated by solution of the inverse problem, permits the determination of the constants C_1 and C_2 in each finite element. These constants may then be used in the analysis of response to other earthquakes.

DYNAMIC ANALYSIS OF MATAHINA DAM

The accelerations and deformations induced in Matahina Dam by the Edgecumbe earthquake are computed using the 2-D finite element program TARA-3 (Finn et al., 1986). Constant strain triangular finite elements were used to model the dam (Fig. 4) because the inverse solution technique used to determine the volumetric strain distribution in the rockfill is, in theory, exact when triangular elements are used. The procedure developed for solving the inverse problem using a modified version of TARA-3 requires a constant modulus over each finite element which is provided by the constant strain triangular elements.

The accelerations recorded near the toe of the downstream shoulder (Fig. 5) were used as input motions for the seismic response analyses.

The first step in the analysis is to establish the stress-strain state in the dam before the earthquake. The seismic loading in TARA-3 analysis will start from this strained state and not from the origin of the stress-strain curve as in conventional methods of dynamic analysis. The initial state is determined using the nonlinear static analysis option in TARA-3 to construct the dam in layers. In the static analysis, the buoyant unit weight was used for all materials below the lake level or the phreatic line. The reservoir water pressures were applied against the core.

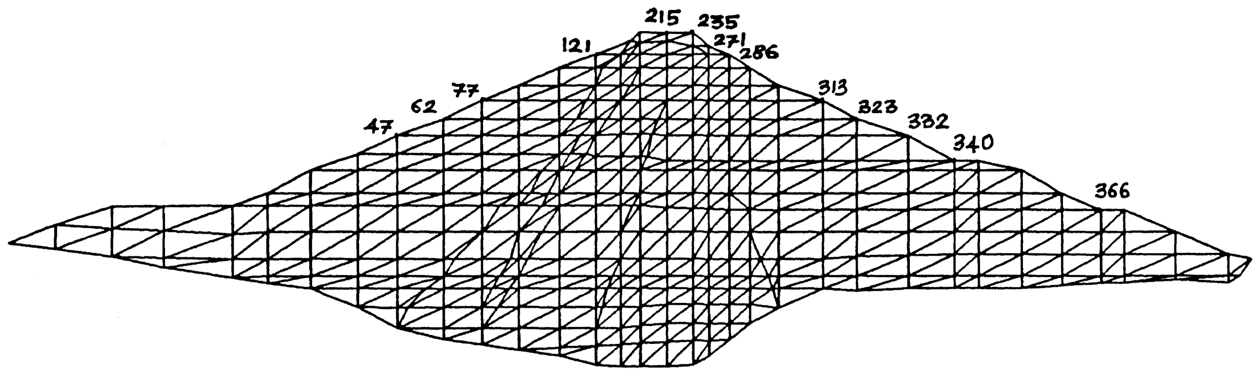

Fig. 4. Finite Element Mesh for Matahina Dam.

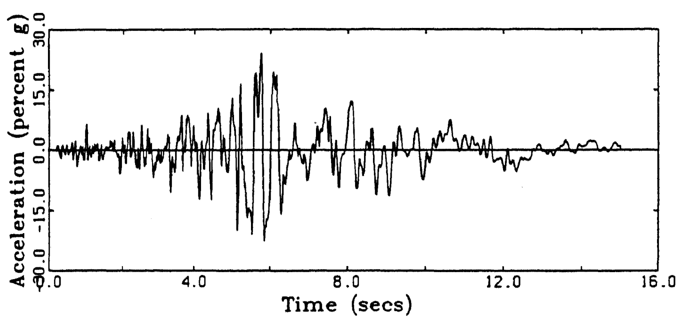

Fig. 5. Acceleration Input for Dynamic Analysis.

Material Properties

The maximum shear moduli in the rockfill and core, consistent with the mean effective stress regime in the dam, σ'_m, were calculated using a modified version of the formula (Seed and Idriss, 1970)

$$G_{max} = 21.7 P_a K_{2max} \left(\frac{\sigma'_m}{P_a} \right)^{0.5} \tag{11}$$

in which P_a is the atmospheric pressure and K_{2max} is a parameter that depends on material type and density. A suitable value for K_{2max} was derived from the shear wave velocity measurements, V_s, at a few locations in the rockfill and in the core. The maximum shear modulus, G_{max}, is given by

$$G_{max} = \rho V_s^2 \tag{12}$$

in which ρ is the mass density. The value of K_{2max} may then be determined by substituting this value of G_{max} in equation (11). This procedure gave an average value of $K_{2max} = 40$ for the rockfill and $K_{2max} = 25$ for the core.

The bulk modulus, B, is given by equation (8), repeated here for convenience,

$$B_t = K_b P_a \left(\frac{\sigma'_m}{P_a} \right)^n \tag{13}$$

in which K_b is the bulk modulus number, and n is the bulk modulus exponent.

For the pre-earthquake construction analysis, $K_b = 1040$, and $n = 0.4$ were used for the rockfill based on values quoted by Duncan et al. (1978). For dynamic analysis in which it was desired to maintain essentially constant volume, values of $K_b = 4120$ and $n = 0.4$ were selected for the rockfill. For the core $K_b = 5420$ and

$n = 0.5$ were used. These values correspond to a Poisson ratio of $\mu = 0.495$. This is the closest approach allowable to the constant volume condition in the computational model.

The strength of the rockfill was expressed conservatively by an effective angle of internal friction $\phi' = 38°$. The undrained shear strength of the core was assumed to vary linearly with mean effective stress σ'_m from the known values near the surface (Lim, 1988).

Procedure for Analysis

The constant volume residual deformations were calculated using the appropriate material parameters in the previous section. This is a reasonable assumption for the behaviour of the core during the earthquake. Therefore the differences between measured and computed deformations could be attributed to volume changes in the rockfill, if the deformation measurements had been made directly after the earthquake. Residual porewater pressures undoubtedly developed in the core and eventually contributed additional displacement after consolidation. Therefore assigning all significant volume changes to the rockfill appears to be a reasonable assumption. However, in the short time between the earthquake and the post-earthquake displacement measurements, significant consolidation in the core is not considered to have taken place. Furthermore, subsequent deformations of the dam suggest that the consolidation deformation of the cone is small compared to the total deformations in the dam.

The volume changes in the rockfill were calculated by applying the measured deformations of the downstream shoulder as boundary conditions to the dam in the state at the end of constant volume distortion. Displacements at finite element nodes on the downstream shoulder at which measurements of post-earthquake deformations had not been measured were estimated by interpolating between nodes with known displacements. The constant volume requirement was relaxed and bulk moduli with parameters $K_b = 1040$ and $n = 0.4$ were used again in the rockfill for the inverse analysis.

From the computed volumetric strains and the shear strain history in each finite element, the constants C_1 and C_2 may be calculated for each element on the basis of equation (9) using the program SIMCYC (Yogendrakumar and Finn, 1986). This is an extensive computational exercise. It seems adequate to determine C_1 and C_2 for blocks of adjacent elements.

The procedure for subsequent analyses was now tested by re-calculating the response of the Matahina Dam to excitation by the Edgecumbe earthquake using the measured material properties and the computed volume change characteristics of the rockfill. For this dynamic analyses four node quadrilateral isoparametric finite elements were used. This forward solution process, because of approximations in the method, does not give the measured displacements exactly, particularly near the crest where the incremental strains are largest.

SELECTED RESULTS OF ANALYSIS

The computed and measured accelerations near mid-height at station C agree fairly well with the measured response (Fig. 6). Some of the high frequency noise was filtered out of the recorded acceleration by filtering out frequencies higher than 5 Hz. The major difference between the recorded and computed accelerations is the sharp negative spike in the recorded response. However, single narrow spikes of this kind have no effect on the overall stability or displacement patterns in an earth or rockfill embankment.

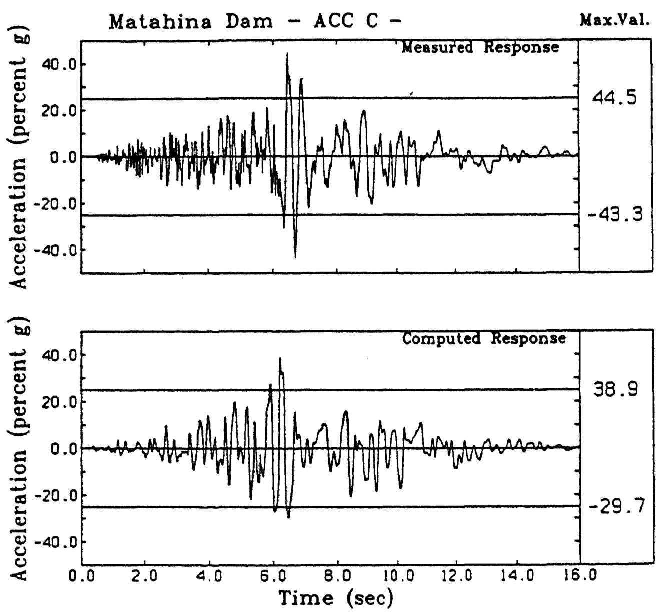

Fig. 6. Comparison of Measured Acceleration at Mid-Height of Matahina Dam Filtered Above 5 Hz with Computed Accelerations.

Time histories of vertical and horizontal displacements node 235 on the downstream shoulder are shown in Figs. 7 and 8. The plots show the sharp increases in horizontal and vertical displacements with the advent of strong shaking around time t=6 seconds. The residual displacements are dominant. Transient cyclic displacements

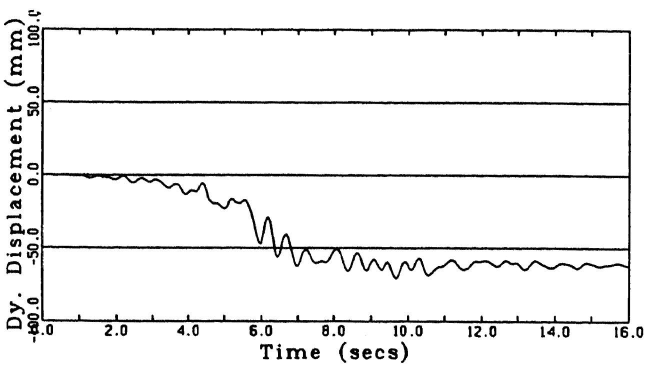

Fig. 7. Time History of Dynamic Vertical Displacement of Node 235 on the Downstream Slope of Matahina Dam.

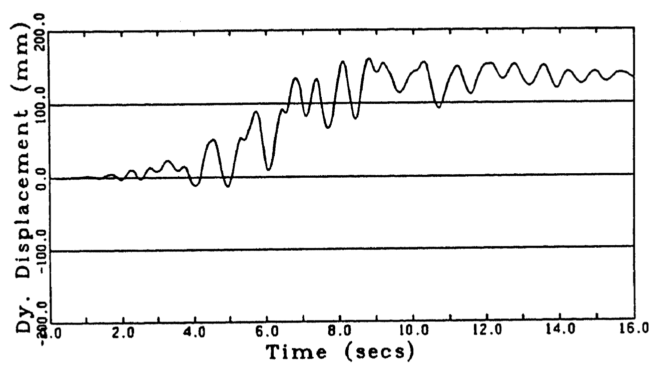

Fig. 8. Time History of Dynamic Horizontal Displacement of Node 235 on the Downstream Slope of Matahina Dam.

matching the cyclic nature of the input are negligible in comparison with the large residual displacements due to hysteretic action. The residual displacements reach a constant value after the segment of strongest shaking from about 6 to 9 seconds. Thereafter the excitation merely results in unloading and reloading below pervious loading levels so the response is essentially elastic with little further increase in permanent displacements.

Technically the response is trapped in smaller hysteretic loops embedded in the larger loops established by the very strong shaking between 6 and 9 seconds after the earthquake started. This results in essentially elastic response.

Table 1 shows excellent agreement between computed and measured displacements except for the vertical component of displacement of the crest. The reason for this discrepancy is not known but it is probable that more refined modelling is needed near the crest.

Table 1. Comparison of Measured and Computed Seismic Displacements of Matahina Dam in mm

Node	X_{meas}	X_{comp}	Y_{meas}	Y_{comp}
215	-	85	- 34	- 44
235	268	234	-102	- 99
271	164	153	- 92	- 88
323	90	98	- 58	- 53
340	51	54	- 42	- 41
366	33	33	- 22	- 22
202	-	10	- 11	- 5

Further tuning of the properties can be done to achieve a closer match but for analysis of dam stability and determining the permanent deformations under a larger design earthquake such a refinement seems neither necessary nor cost-effective.

ST. JOE STATE PARK TAILINGS DAM

Two tailings dams were constructed by the St. Joe Lead Company near Flat River, Missouri, from 1911 to 1965. These dams are designated Original Dam and Main Dam. When the mine closed, the entire processing facility was donated to the State of Missouri. The dams are situated within the zone of influence of the 1811-1812 New Madrid earthquakes. An assessment of the seismic stability of these tailings dams was conducted in 1990 (Vick et al., 1992). This paper describes some of the effective stress nonlinear dynamic analyses and flow deformation analyses conducted on the Original Dam. An idealized section of the Original Dam is shown in Fig. 9.

The properties used in static and dynamic analyses of the Original Dam are based on engineering judgement and on representative $(N_1)_{60}$ values selected from boring logs and corrected when necessary for fines content.

The liquefaction resistances of the materials in the dam against the design earthquake were obtained using the liquefaction resistance curve developed by Seed et al. (1985). The resistances so obtained were corrected for overburden pressure and for the initial static shear-stress ratio τ_{st}/σ'_{vo} using the correction factors K_σ and K_α given by Seed and Harder (1990).

Complete liquefaction resistance curves for each material type were determined by entering the curves in Fig. 10 with the appropriate $(N_1)_{60}$ value (Koester and Franklin, 1985). The liquefaction resistance corresponding to each earthquake magnitude was associated with the corresponding number of cycles taken from Table 2. The liquefaction resistance curve for the lower slimes obtained in this way is shown in Fig. 11.

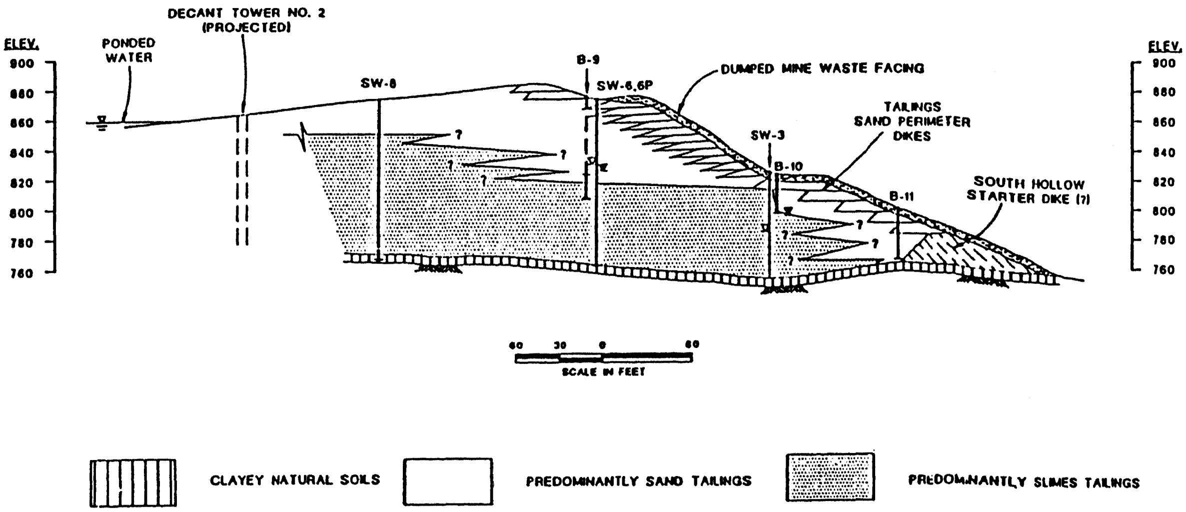

Fig. 9. Idealized Section of Original Dam

Table 2. Loading Cycles as a Function of Earthquake Magnitude (Seed and Harder, 1990)

Magnitude	No. of Cycles
8	26
7.5	15
6.75	10
6.0	5-6
5.25	2-3

The volume change parameters C_1, C_2 and $\overline{E}_r$ in the porewater pressure generation model in TARA-3 were selected to model the specified liquefaction resistances. The smooth curve in Fig. 11 is the simulation by the TARA-3 model and the points are the resistances derived from Fig. 10.

Dynamic Effective Stress Analysis

The finite element mesh used for analyses of the Original dam is shown in Fig. 12. The distribution of materials in the dam for analysis was an idealized version of that shown in Fig. 9.

The peak ground acceleration was specified by the client as 0.2 g. For the preliminary screening study of liquefaction potential, the S69E component of the Kern County earthquake (1952) M = 7.2 recorded at the Taft-Lincoln School tunnel was used as input motion for the dynamic analysis. The record was scaled to a peak

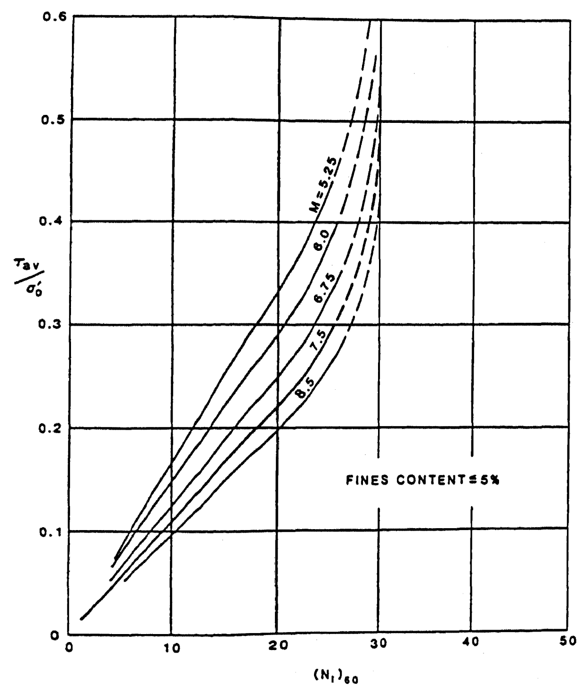

Fig. 10. Liquefaction Resistance Assessment Chart (from Koester and Franklin, 1985).

acceleration of 0.2 g and the first 15 seconds of the record was used.

The accelerations at node 39 are shown in Fig. 13. This node is located in the lower slimes which do not liquefy during the earthquake. The porewater pressure

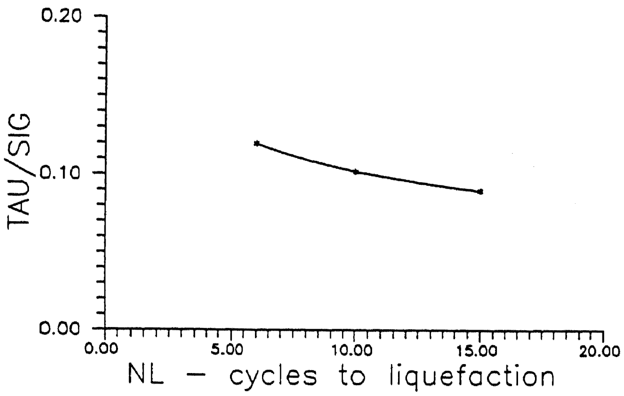

Fig. 11. Liquefaction Resistance of Lower Slimes.

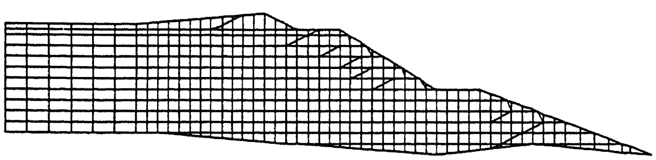

Fig. 12. Finite Element Mesh for the Original Dam.

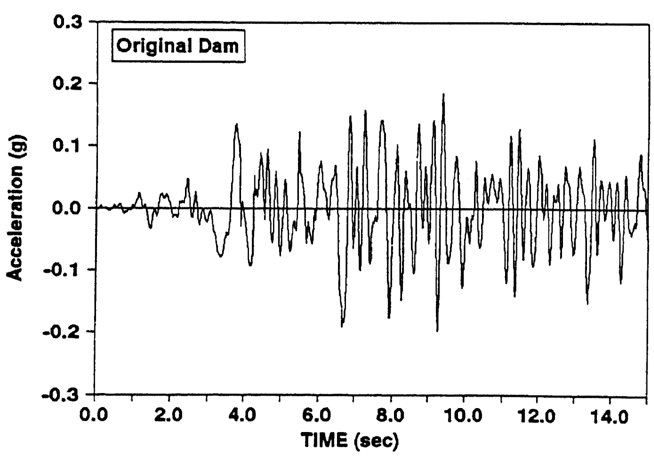

Fig. 13. Original Dam; Acceleration Time History at Node 39 in Non-Liquefied Region of Dam.

development in elements below node 39 is typified by the porewater pressures in element 36 shown in Fig. 14. Note the strong acceleration response over the entire record from 4 seconds to 15 seconds.

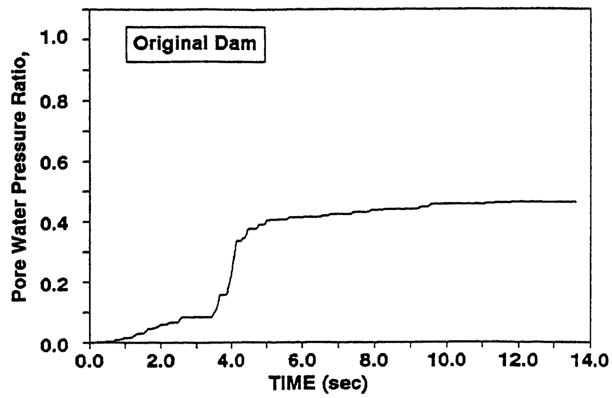

Fig. 14. Original Dam; Pore Pressure Ratios in Element 36 in Lower Slimes Which Do Not Liquefy.

The accelerations at node 45 are shown in Fig. 15. This node is underlain by the upper slimes which liquefied during the earthquake. The porewater pressures in element 88 which underlies node 45 are shown in Fig. 16. Note that the slimes liquefy after about 5 seconds. The effect of liquefaction on the accelerations at node 45 are clearly evident. The response after about 7 seconds is greatly attenuated compared with the very strong acceleration response after 7 seconds at node 39 (Fig. 13).

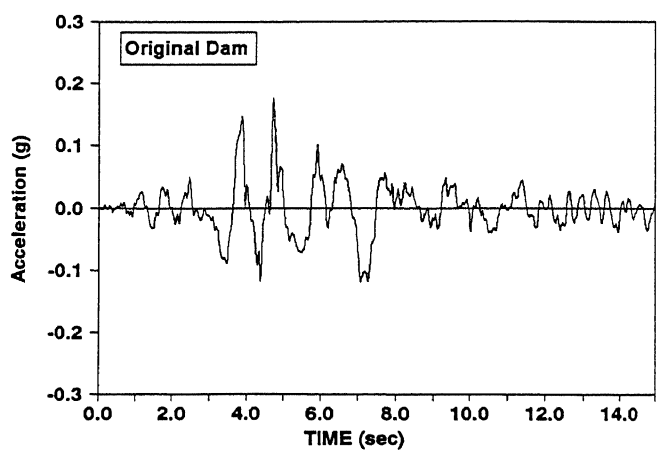

Fig. 15. Original Dam; Acceleration Time History at Node 45 Over Liquefied Upper Slimes.

POST-LIQUEFACTION ANALYSIS OF ORIGINAL DAM

An important consideration in evaluating the seismic stability of an earth structure such as an embankment dam with potentially liquefiable materials is whether a flow failure will occur after liquefaction. This will

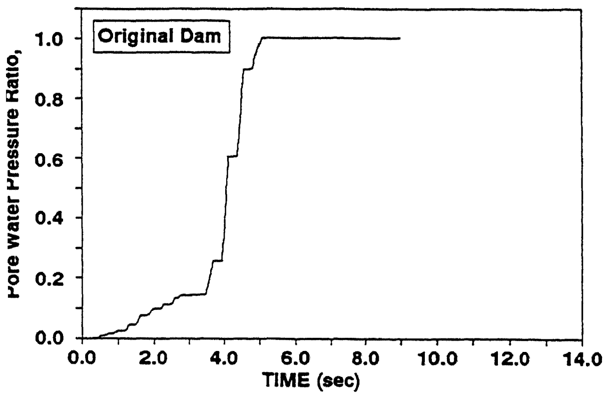

Fig. 16. Original Dam; Pore Pressure Ratios in Element 88 in Upper Slimes Showing Liquefaction after 5 s.

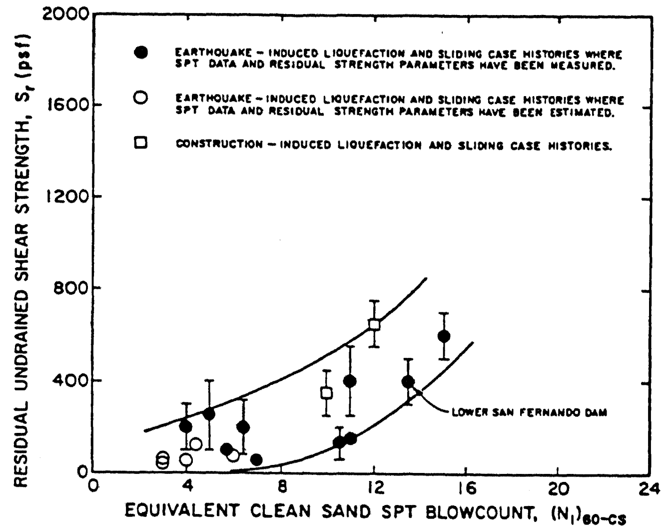

Fig. 17. Relationship Between Residual Strength and SPT N Values for Sands (Seed and Harder, 1990).

depend on the relationship between the average driving shear stresses in the dam along any potential failure surface and the corresponding steady state or residual strengths of the liquefied materials (Castro et al., 1985). Liquefaction in this context is synonymous with strain softening of soil in undrained shear. When the soil is strained beyond the point of peak strength, the undrained strength drops to a value that is maintained constant over a large range in strain. This is called the undrained steady state or residual strength. If the driving shear stresses due to gravity on a potential slip surface through liquefied materials in an embankment are greater than the undrained residual strength, deformations will occur until the driving stresses are reduced to values compatible with static equilibrium. The more the driving stresses exceed the steady state strength, the greater the deformations to achieve equilibrium.

Residual strength of the liquefied materials in the Original Dam were determined using the correlation between residual strength and $(N_1)_{60}$ developed originally by Seed (1987) and updated by Seed and Harder (1990). The residual strengths used in evaluating the stability of the Original Dam are based on representative $(N_1)_{60}$ values for the potentially liquefiable materials and the lower bound curve of the Seed and Harder (1987) correlation (Fig. 17).

The liquefaction resistance of the lower slimes depends heavily on a 100% increase in measured $(N_1)_{60}$ as a correction for fines content. With the average porewater pressure ratio in these slimes running about 50%, it would not be prudent to rely on the correction to prevent liquefaction considering the limited data on in-situ penetration resistance and the uncertainty associated with fines corrections at very low $(N_1)_{60}$ values. Therefore, in these preliminary deformation studies the residual strength was assumed to be triggered in the lower slimes.

The lower bound residual strengths for the upper slimes were found to be 50 psf, and for the lower slimes to be 150 psf.

The deformation analysis began from the initial stress state of the dam before the earthquake. The undrained strengths of the liquefiable materials were reduced continuously from their initial values and the resulting deformations of the dam were tracked using the program TARA-3FL (Finn and Yogendrakumar, 1989).

Structure of the Program TARA-3FL

The basic theory of the finite element program TARA-3 has been presented earlier. Only procedures specific to TARA-3FL will be described here. The first requirement is a triggering criterion to switch the strength of any liquefiable element in the dam to the steady state strength at the proper time during the dynamic analysis. Two criteria are available, the peak strain criterion of Castro et al. (1989) and the stress ratio criterion of Vaid and Chern (1985). It is also possible to assume that the residual strength will be triggered in all elements that will liquefy according to the criteria developed by Seed (1983) and Seed et al. (1985) and then concentrate on post-liquefaction behaviour only. This is the procedure that has been followed so far in applying the TARA-3FL analysis in preliminary studies of the remediation of Sardis Dam.

In a particular element in the dam, the shear stress-shear strain state which reflects pre-earthquake conditions is specified by a point P_0 on the stress-strain curve as shown in Fig. 18. When liquefaction is triggered, the

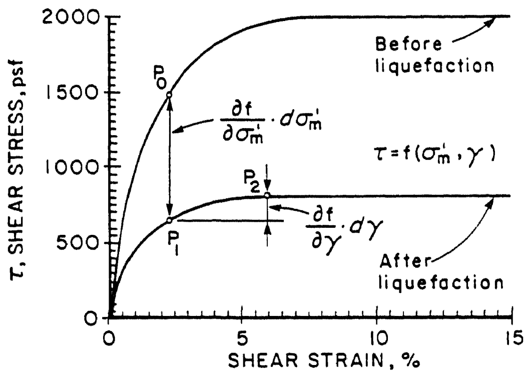

Fig. 18. Adjusting Stress-Strain State to Post-Liquefaction Conditions.

strength will drop to the steady-state value. The post-liquefaction stress-strain curve cannot now sustain the pre-earthquake stress-strain condition and the unbalanced shear stresses are redistributed throughout the dam. In the liquefied elements, the stresses are adjusted according to the following equation,

$$\partial \tau = \frac{\partial f}{\partial \sigma'_m} d\sigma'_m + \frac{\partial f}{\partial \gamma} d\gamma \qquad (14)$$

where $\tau = f(\sigma'_m, \gamma)$. This process leads to progressive deformation of the dam until equilibrium is reached at the state represented by P_2.

Since the deformations may become large, it is necessary to update progressively the finite element mesh. Each calculation of incremental deformation is based on the current shape of the dam, not the initial shape as in conventional finite element analysis. An independent assessment of the equilibrium of the final position should be conducted using a conventional static stability analysis. The factor of safety determined in this way should be unity or greater depending on whether the deformations occurred relatively slowly after the earthquake or during it when inertia forces were acting.

Analysis of Flow Deformations

The progress of deformations as the shear strength drops towards the residual value may be observed by comparing the deformed shapes of the dam in Figs. 19 and 20. In this analysis, the residual strengths of the upper and lower slimes, consistent with Seed's lower bound curve, are 50 psf and 150 psf, respectively.

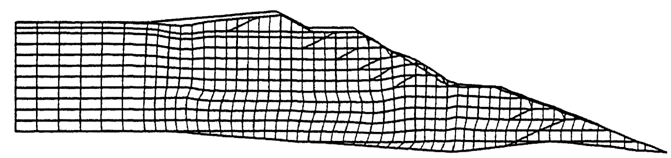

Fig. 19. Original Dam; Deformed Shape when Current Shear Strength of Slimes is 60% of Peak Strength. S_{us} (Upper Slimes) = 50 psf, S_{us} (Lower Slimes) = 150 psf.

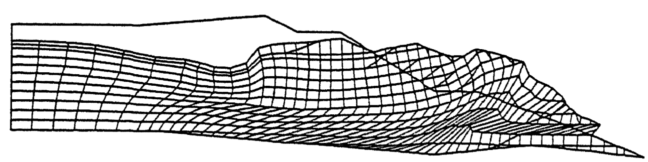

Fig. 20. Original Dam; Deformed Shape when Current Shear Strength of Slimes is 45% of Peak Strength. S_{us} (Upper Slimes) = 50 psf, S_{us} (Lower Slimes) = 150 psf.

Figure 19 shows the deformed shape when the undrained strength in the slimes has dropped to 60% of the original peak value. Although substantial deformations have occurred the dam still maintains its integrity. However, when the strength drops to 45% of the original undrained strength, massive deformations occur as shown in Fig. 20. This failure occurs long before the residual strengths are reached in all liquefiable elements.

CONCLUSIONS

The analysis of the response ,of Matahina Dam to the Edgecumbe earthquake using TARA-3 gave close agreement between measured and computed accelerations and displacements. The analysis uses fully what is known about the material properties of the embankment materials and calculates what is unknown, in this case the volume change characteristics of the rockfill, by using the recorded data on permanent displacements. This is accomplished by solving the inverse problem of determining the volume changes necessary to achieve the additional displacements required to change the constant volume distortions of the dam during the earthquake to the final measured configuration.

The analysis of Matahina Dam under excitation by a suitable design earthquake can now be conducted using the properties determined in the present study.

The analysis of the St. Joe State Park Original Dam demonstrated the capability of nonlinear effective stress analysis to estimate seismically induced porewater pressures and to take the effects of these pressures into account during the analysis. The effect of the porewater pressures is clearly seen by comparing the acceleration records at locations overlying both liquefied and unliquefied materials. The post-liquefaction flow deformation analysis show the capability to track very large deformations and to give a comprehensive picture of the consequences of liquefaction.

The above examples demonstrate that sophisticated finite element analysis has an important place in geotechnical engineering practice, particularly in the detailed interpretation of field performance and the analysis of the behaviour of structures containing liquefiable zones.

ACKNOWLEDGEMENTS

The studies on the behaviour on Matahina Dam were conducted under the general direction of Murray Gillon, Works & Development Services Corp., New Zealand Ltd. The contributions of M. Gillon and C.J. Newton in establishing the in-situ condition of the dam before and after the earthquake is gratefully acknowledged. The preliminary studies of the St. Joe State Park tailings dams were part of a general seismic safety assessment of these dams conducted in collaboration with Steven G. Vick, Consulting Engineer, and Robert Dorey, Steffen Robertson & Kirsten (US).

REFERENCES

Byrne, P.M. (1991), "A Cyclic Shear-Volume Coupling and Pore Pressure Model for Sand", Proc., 2nd Int. Conf. on Recent Advances in Geotech. Earth. Eng. & Soil Dynamics, University of Missouri, Rolla, March 11-15, Vol.I, 47-56.

Duncan, J.M., P.M. Byrne, K.S. Wong and P. Mabry (1978), "Strength, Stress-Strain and Bulk Modulus Parameters for Finite Element Analyses of Stresses and Movements in Soil Masses", Report No. WCB/GT/78-02 to the National Sci. Foundation.

Finn, W.D. Liam (1988), "Dynamic Analysis in Geotechnical Engineering", Earth. Eng. & Soil Dynamics II - Recent Advances in Ground Motion Evaluation, Geotech. Special Publication No. 20, ASCE, August.

Finn, W.D. Liam, W.K. Lee and G.R. Martin (1976), "An Effective Stress Model for Liquefaction", J. of the Geotech. Eng. Div., ASCE, Vol.103, No.GT6, Proc. Paper 13008.

Finn, W.D. Liam, M. Yogendrakumar, N. Yoshida and H. Yoshida (1986), "TARA-3: A Program to Compute the Response of 2-D Embankments and Soil-Structure Interaction Systems to Seismic Loadings", Dept. of Civil Eng., University of British Columbia, Vancouver, Canada.

Finn, W.D. Liam, M.D. Gillon, M. Yogendrakumar and C.J. Newton (1992), "Simulating the Response of a Rockfill Dam", Proceedings, NUMOG IV, Edited by G.N. Pande and S. Pietrusczak, A.A. Balkema, Rotterdam/Brookfield, Vol. 1, pp. 379-393.

Gillon, M.D. (1988), "The Observed Seismic Behaviour of the Matahina Dam", Proc., 2nd Int. Conf. on Case Histories in Geotech. Eng., St. Louis, Missouri, Paper No. 4.29.

Gillon, M.D. and C.J. Newton (1989), "Earthquake Effects at the Matahina Dam in New Zealand", Preprint for Proc., Int. Conf. on Soil Mech. & Found. Eng., Rio de Janeiro, Brazil.

McVerry, G.H. (1987), "Linear Modal Analysis of the Response of Matahina Dam in the Edgecumbe Earthquake", Report prepared for the Power Div., Ministry of Works & Development, Physics & Eng. Laboratory, DSIR, Lower Hutt.

McVerry, G.H. (1989). Private Communication.

Martin, G.R., W.D. Liam Finn and H.B. Seed (1975), "Fundamentals of Liquefaction Under Cyclic Loading", J. of the Geotech. Eng. Div., ASCE, Vol. 101, GT5, Proc. Paper 11284.

Masing, G. (1926), "Eigenspannungen und Verfestigung beim Messing", Proc., 2nd Int. Congress of Applied Mechanics, Zurich, Switzerland.

Seed, H.B. (1987), "Design Problems in Soil Liquefaction", J. of Geotech. Eng., ASCE, Vol. 3, No. 12, December.

Seed, H.B. and I.M. Idriss (1970), "Soil Moduli and Damping Factors for Dynamic Response Analyses", Report No. EERC-70-10 Earth. Eng. Res. Center, University of California, Berkeley, CA, December.

Staff, New Zealand Department of Scientific and Industrial Research, (1987), The March 2, 1987 Earthquake Near Edgecumbe, North Island, New Zealand. EOS, Transactions, American Geophysical Union, Vol.68, No.44, Nov. 3.

Sutherland, A.J. and T.C. Logan (1988), "Matahina Dam: Shear Wave Testing of Construction Materials", Central Laboratories Report 88-B2313 Lower Hutt, New Zealand.

Vick, S.G., R. Dorey, W.D. Liam Finn and R.C. Adams (1992), "Seismic Stabilization of St. Joe Park Tailings Dams", submitted for review.

Yogendrakumar, M. and W.D. Liam Finn (1986), "SIMCYC: A Program for Simulating Cyclic Simple Shear Tests on Dry or Saturated Sands", Report, Soil Dynamics Group, Dept. of Civil Eng., University of British Columbia, Vancouver, Canada.